Acta Geod Geophys (2017) 52:301–316
DOI 10.1007/s40328-016-0189-x

ORIGINAL STUDY

# A noise analysis method for GNSS signals of a standalone receiver

**Zhetao Zhang[1] · Bofeng Li[1] · Yunzhong Shen[1] · Ling Yang[1]**

Received: 11 August 2016 / Accepted: 3 November 2016 / Published online: 18 November 2016


**Abstract** Extensive studies on signal noise analysis of Global Navigation Satellite Systems (GNSS) receivers are mainly based on zero and/or short baselines where a pair of receivers is required. This paper develops a new signal noise assessment method for a standalone GNSS receiver. In this new method, the time differenced geometry-free (ΔGF) model is formed, where the residual ionospheric delay and multipath remain. In order to eliminate these systematic trend biases, the second-order polynomial fitting is used. Then the mixed autoregressive moving average (ARMA) model is further applied to capture this stationary and time-correlated time series. As a result, the pure random noise of ΔGF is obtained, which is finally used to assess the precision of receiver signal in terms of the error propagation law. The performance of this new method is numerically tested by using 10 sets of data and compared with the methods of zero and short baselines. The results indicate that the new method is able to assess both the phase and code precision of a standalone receiver, and the conclusions are consistent to those from the methods of zero and short baselines. Since again the new method needs only one receiver, it could be implemented in more applications than the traditional methods, especially in precise point positioning.

**Keywords** GNSS receiver · Signal noise · Time correlation · Geometry-free model · ARMA model

✉ Bofeng Li
bofeng_li@tongji.edu.cn

[1] College of Surveying and Geo-Informatics, Tongji University, Shanghai 200092, People's Republic of China

## 1 Introduction

The precise point positioning (PPP) based on Global Navigation Satellite Systems (GNSS) observations has been extensively studied in recent years, where a standalone receiver is involved for the precise positioning (Zumberge et al. 1997; Ge et al. 2008). Selecting the appropriate receiver is a critical issue (Rodríguezpérez et al. 2007) and the precision of observations is indispensable for setting up a stochastic model (Wang et al. 2002). Without realistic stochastic model, one cannot obtain the optimal PPP solutions as well as more importantly an objective measure of PPP solutions.

A number of researchers have studied the precision evaluation of GNSS receiver measurements in recent years. The most widely used methods are based on zero and short baseline where a pair of receivers is involved. Hereafter those are referred to as the zero and short baseline methods. In zero baseline method, two receivers (usually with the same type) are connected to the same antenna (including low-noise amplifier) (Nolan et al. 1992; Van der Marel et al. 2009) and the baseline elements are all known as zero. In this case, the common external errors, such as atmospheric biases, and multipath etc., can be completely eliminated in manner of single differenced observations, and only the signal noise remains (Bona and Tiberius 2000). The drawback of the zero baseline method is that it can only evaluate signal noise attributed to the receiver since the signal noise attributed to the antenna is completely eliminated (too optimistic results). In the short baseline method, two receivers are connected to two antennas spaced by a very short distance, typically several meters, such that again the common external errors can be significantly eliminated. However, different from the zero baseline method, two antennas are involved in the short baseline method, which allow evaluating the signal noise attributed to not only receivers but also antennas. That is the one reason why the observation precision obtained from zero baseline method are more easily higher than those from the short baseline method (de Bakker et al. 2009, 2012). Hence the short baseline method can be applied as a complementary to the zero baseline method. The disadvantage of the short baseline method with respect to the zero baseline method is that the remaining unmodeled errors, mainly the multipath, could not be ignored. In order to retrieve the pure observation noise, additional data processing operations should be further applied (Amiri-Simkooei and Tiberius 2007; de Bakker et al. 2009).

While much research has been devoted on evaluating the signal noise on the basis of a relative mode, little research has been done with a standalone receiver. In the PPP applications, the stochastic model set-up is normally based on the knowledge obtained from the zero/short baseline method (Afifi and El-Rabbany 2013). However, if the two tested receivers do not have the same performance although with the common type, one cannot obtain the true precision of receiver signals. Moreover, the method of traditional standalone receiver signal noise assessment is based on the time differenced operator without taken into consideration the integrated time correlation. Specifically, not only the mathematical correlations exist due to the operation, but also the physical correlations exist from the unmodeled errors of the signal itself (El-Rabbany 1994; Howind et al. 1999). Therefore, it is essential to develop a stable and mature method for evaluating the signal noise of a standalone receiver.

In this research, we propose a noise assessment method for GNSS signal noise with a standalone receiver. The key of this new method is how to extract the pure signal noise by properly eliminating all systematic errors. We first form the time differenced geometry-free ($\Delta$GF) model to eliminate all geometry-specific errors. Then we apply the second-order

polynomial fitting to remove remained systematic biases of ionospheric delay and multipath in detrended ΔGF observations. This two-step processing results in bias-free but time-correlated ΔGF observations. The time correlations are attributed to mathematical and physical correlations. Then a mixed autoregressive moving average (ARMA) model is further used to capture the noise of ΔGF, where the time correlations are fully taken into account. Finally, the signal precision is estimated by means of the error propagation law.

## 2 Methodology

### 2.1 The ΔGF model

The GNSS observation equations of phase and code from receiver $r$ to satellite $s$ on frequency $i$ read (Leick et al. 2015)

$$\phi^s_{r,i} = \rho^s_r + c\delta t_r - c\delta t^s + \lambda_i N^s_{r,i} - I^s_{r,i} + T^s_r + m^s_{r,i} + \zeta_{r,i} - \zeta^{s,i} + \varepsilon^s_{r,i} \tag{1}$$

$$P^s_{r,i} = \rho^s_r + c\delta t_r - c\delta t^s + I^s_{r,i} + T^s_r + M^s_{r,i} + \xi_{r,i} - \xi^{s,i} + e^s_{r,i} \tag{2}$$

where $\phi^s_{r,i}$ and $P^s_{r,i}$ are the phase and code observations, respectively; $\rho^s_r$ is the receiver-to-satellite range; $c$ is the speed of light in a vacuum; $\delta t_r$ and $\delta t^s$ are the receiver and satellite clock errors, respectively; $\lambda_i$ is the wavelength of the $i$-th frequency; $N^s_{r,i}$ is the integer ambiguity; $I^s_{r,i}$ is the ionospheric delay; $T^s_{r,i}$ is the tropospheric delay; $m^s_{r,i}$ and $M^s_{r,i}$ are the multipath effects of phase and code, respectively; $\zeta_{r,i}$ and $\zeta^{s,i}$ are the phase hardware delays with respect to receiver and satellite, respectively; $\xi_{r,i}$ and $\xi^{s,i}$ are the code hardware delays for receiver and satellite, respectively; $\varepsilon^s_{r,i}$ and $e^s_{r,i}$ are the random errors of phase and code, respectively.

According to (1) and (2), two types of geometry-free (GF) models from the receiver $r$ to satellite $s$ on frequencies $i$ and $j$ can be calculated as follows

$$\mathrm{GF1}_{i,j} =: \phi^s_{r,i} - \phi^s_{r,j} = \lambda_i N^s_{r,i} - \lambda_j N^s_{r,j} - \left(1 - \lambda_j^2 \Big/ \lambda_i^2\right) I^s_{r,i} + m^s_{r,\mathrm{GF1}} + \zeta_{r,\mathrm{GF1}} - \zeta^{s,\mathrm{GF1}} + \varepsilon^s_{r,\mathrm{GF1}} \tag{3}$$

$$\begin{aligned} \mathrm{GF2}_i =: P^s_{r,i} - \phi^s_{r,i} &= 2I^s_{r,i} - \lambda_i N^s_{r,i} + M^s_{r,i} - m^s_{r,i} + \xi_{r,i} - \xi^{s,i} - \zeta_{r,i} + \zeta^{s,i} + e^s_{r,i} - \varepsilon^s_{r,i} \\ &\approx 2I^s_{r,i} - \lambda_i N^s_{r,i} + M^s_{r,i} + \xi^s_{r,i} - \zeta^s_{r,i} + e^s_{r,i}. \end{aligned} \tag{4}$$

Because the GNSS signals from the same satellite have almost the same propagation path, the majority of error sources will be eliminated by the time differenced operator (Hofmann-Wellenhof et al. 2007). Only the GF1 model contains the ambiguities on frequencies $i$ and $j$, ionospheric delay, multipath, hardware delays and random errors for phase. In the GF2 model, the multipath and phase noise are much smaller than those of code, then consequently neglected. Therefore, only the ambiguities on frequency $i$ or $j$, ionospheric delay, multipath, phase and code hardware delays and code random errors remain. If the GF($t$) and GF($t + 1$) are calculated at the epoch of $t$ and $t + 1$, the ΔGF model is mathematically defined as

$$\Delta\mathrm{GF}(t) =: \mathrm{GF}(t{+}1) - \mathrm{GF}(t). \tag{5}$$

Based on (3) and (4), in absence of cycle slips, the constant ambiguities are removed. Besides, the hardware delays are eliminated, and the ionospheric delay and multipath are reduced. There only leave residual ionospheric delay, multipath and random errors. According to (3) and (4), two types of ΔGF can be expressed as

$$\begin{aligned}\Delta \mathrm{GF1}_{i,j}(t) =: \mathrm{GF1}_{i,j}(t+1) - \mathrm{GF1}_{i,j}(t) = \Delta\left(\lambda_j^2 \Big/ \lambda_i^2 - 1\right) I_{r,i}^s(t) + \Delta m_{r,\mathrm{GF1}}^s(t) \\ + \Delta \varepsilon_{r,\mathrm{GF1}}^s(t)\end{aligned} \tag{6}$$

$$\Delta \mathrm{GF2}_i(t) =: \mathrm{GF2}_i(t+1) - \mathrm{GF2}_i(t) = 2\Delta I_{r,i}^s(t) + \Delta M_{r,i}^s(t) + \Delta e_{r,i}^s(t) \tag{7}$$

where the other terms are the same as those defined previously.

## 2.2 Process of ΔGF model

Generally, the residual ionospheric delay and multipath are low frequency signals compared with the signal noise, hence they will have a slight trend (Tiberius et al. 2001; de Bakker et al. 2009, 2012). This trend term can be handled by low order polynomials if the time span is not too long (e.g. less than 3 h). Therefore, a constant, a linear, or a second order polynomial can be used to fit the ΔGF observations and then remove the systematic trend. The parameters of the polynomial fitting model are solved by the least squares (LS) method. In this paper, a second-order polynomial is chosen. Accordingly, the trend term of ΔGF ($\Delta \mathrm{GF}_t$) is given as

$$\Delta \mathrm{GF}_t = \alpha_1 + \alpha_2 \times t + \alpha_3 \times t^2 \tag{8}$$

where $\alpha_1$, $\alpha_2$ and $\alpha_3$ are the parameters to be estimated; $t$ is the epoch number. Hence, the detrended ΔGF ($\Delta \mathrm{GF}_d$) time series can be obtained by subtracting the $\Delta \mathrm{GF}_t$ from ΔGF, thus becoming a stationary time series.

It follows from (5) that the ΔGF observations contain the GNSS signals of consecutive epochs, which will result in mathematical correlations. Besides, there also exist physical correlations due to the unmodeled errors in GNSS data (El-Rabbany 1994; Howind et al. 1999). Therefore we need a technique that can correctly describe such time-correlated process in order to extract the pure random noise $v(t)$ of ΔGF. The $\Delta \mathrm{GF}_d$ time series can be treated by an ARMA model, which provides a description of a stationary process in terms of two polynomials (Chatfield 1984; Box et al. 1994; Hamilton 1994).$\Delta \mathrm{GF}_d$ ($t$-1), $\Delta \mathrm{GF}_d$ ($t$-2),…, $\Delta \mathrm{GF}_d$ ($t$-$p$) are the autoregressive terms and $v(t\text{-}1)$, $v(t\text{-}2)$,…, $v(t\text{-}q)$ are the moving average terms. Hence the preprocessed ΔGF can be regarded as ARMA($p$,$q$) model. The $\Delta \mathrm{GF}_d$ is then given as

$$\Delta \mathrm{GF}_d(t) = f(t)\beta + v(t) \tag{9}$$

with

$$f(t) = \left[\Delta \mathrm{GF}_d(t-1), \Delta \mathrm{GF}_d(t-2), \cdots, \Delta \mathrm{GF}_d(t-p), v(t-1), v(t-2), \cdots, v(t-q)\right]$$

$$\beta = \left[\varphi_1, \varphi_2, \cdots, \varphi_p, \theta_1, \theta_2, \cdots, \theta_q\right]^{\mathrm{T}}$$

where $\varphi_1$,…, $\varphi_p$ are the autoregressive parameters; $\theta_1$,…, $\theta_q$ are the moving average parameters. If there are $K$ epochs, the multi-epoch model can be formed

$$Y(K) = F(K)\beta + V(K) \tag{10}$$

with

$$Y(K) = [\Delta \mathrm{GF}_d(t), \Delta \mathrm{GF}_d(t+1), \cdots, \Delta \mathrm{GF}_d(K)]^{\mathrm{T}}$$

$$F(K) = [f(t), f(t+1), \cdots, f(K)]^{\mathrm{T}}$$

$$V(K) = [v(t), v(t+1), \cdots, v(K)]^{\mathrm{T}}.$$

Now the LS solutions of these $K$ epochs can be derived as

$$\hat{\beta} = \left[F^{\mathrm{T}}(K)F(K)\right]^{-1} F^{\mathrm{T}}(K)Y(K) \tag{11}$$

Because $f(t)$ depends on the previous epochs, an iterative estimation procedure is required.

In practice, there are many choices of ARMA($p$,$q$) model orders in (10). Therefore, the most appropriate orders of autoregressive and moving average parameters should be determined from the alternative choices. Then a criterion to measure quantitatively the model quality is applied. In this study, the Bayesian information criterion (BIC) is used, which is defined as (Schwarz 1978):

$$\mathrm{BIC}\left(\hat{\beta}\right) = -2l + (p+q) \times \ln K \tag{12}$$

where $l$ is the optimized log likelihood objective function value associated with the parameter estimates; other terms in (12) are the same as those defined previously. The best order is chosen when one certain set of parameters $\hat{\beta}$ obtain the minimum BIC value.

In the end, the random noise of ΔGF can be estimated as

$$\hat{V}(K) = Y(K) - F(K)\hat{\beta}. \tag{13}$$

### 2.3 Determination of signal noise

In order to determine the signal precision, the standard deviation (STD) of ΔGF random noise is calculated first. Then to obtain the unbiased estimation, the corrected sample STD (Welford 1962) is given by:

$$\sigma_v = \sqrt{\frac{\sum_{t=1}^{K} (v(t) - \overline{v})^2}{(K-p) - (p+q)}} \tag{14}$$

where $\overline{v}$ is the mean value of ΔGF random noise over $K$ epochs, and all the terms in (14) are the same as those defined previously.

According to the error propagation law, the signal precision can be estimated. For the GF1 model, the signal precision can be calculated as follow when using the $i$-th and $j$-th frequencies for one certain satellite:

$$\sigma_{v_1}^2(t) = \sigma_{\varepsilon_i}^2(t+1) + \sigma_{\varepsilon_i}^2(t) + \sigma_{\varepsilon_j}^2(t+1) + \sigma_{\varepsilon_j}^2(t) \tag{15}$$

where $\sigma_{v_1}(t)$ is the STD of the ΔGF1 random noise at the epoch $t$; $\sigma_{\varepsilon_i}(t+1)$ and $\sigma_{\varepsilon_i}(t)$ are the STDs of phase random noise on the frequency $i$ at the epoch $t+1$ and $t$, respectively; $\sigma_{\varepsilon_j}(t+1)$ and $\sigma_{\varepsilon_j}(t)$ are the STDs of phase random noise on the frequency $j$ at the epoch

$t+1$ and $t$, respectively. Because the random noise is independent of time, the $\sigma^2_{\varepsilon_i}(t+1)$ and $\sigma^2_{\varepsilon_i}(t)$, $\sigma^2_{\varepsilon_j}(t+1)$ and $\sigma^2_{\varepsilon_j}(t)$ can be treated equal. Then (15) is derived as

$$\sigma^2_{v_1} = 2\sigma^2_{\varepsilon_i} + 2\sigma^2_{\varepsilon_j}. \tag{16}$$

For one receiver, the precision of phase measurements is related to the wavelength (Han 1997; Langley 1997)

$$\frac{\sigma^2_{\varepsilon_i}}{\sigma^2_{\varepsilon_j}} = \frac{\lambda_i^2}{\lambda_j^2}. \tag{17}$$

Since we can get the $\sigma_{v_1}$ for every satellite, in this study, only the satellites above 35° elevation are applied, which can largely reduce the external influence (Euler and Goad 1991; Bona 2000). Therefore we can use the mean value of $\sigma_{v_1}$ ($\overline{\sigma}_{v_1}$), which is more accurate to substitute the $\sigma_{v_1}$. Finally, the dual frequency carrier phase noise from (16) and (17) can be estimated as:

$$\sigma_{\varepsilon_i} = \frac{\bar{\sigma}_{v_1}}{\sqrt{2\left(1+\lambda_j^2/\lambda_i^2\right)}} \tag{18}$$

$$\sigma_{\varepsilon_j} = \frac{\bar{\sigma}_{v_1}}{\sqrt{2\left(1+\lambda_i^2/\lambda_j^2\right)}}. \tag{19}$$

For the GF2 model and signal frequency $i$, the similar relationship as for the GF1 model is:

$$\begin{aligned}\sigma^2_{v_2}(t) &= \sigma^2_{e_i}(t+1) + \sigma^2_{\varepsilon_i}(t) + \sigma^2_{e_i}(t+1) + \sigma^2_{\varepsilon_i}(t) \\ &\approx 2\sigma^2_{e_i}\end{aligned} \tag{20}$$

where $\sigma_{v_2}(t)$ is the STD of the ΔGF2 random noise at the epoch $t$; $\sigma_{e_i}(t+1)$ and $\sigma_{e_i}(t)$ are the STDs of code random noise on the frequency $i$ at the epoch $t+1$ and $t$, respectively; the other terms in (20) are the same as those defined previously. Because the phase random noise is much smaller than the code random noise, the phase random noise can be ignored.

Analogously, the mean value of $\sigma_{v_2}$ ($\overline{\sigma}_{v_2}$) can be calculated from the satellites of which elevations are higher than 35°. As a result, the noise of the code signal is estimated as

$$\sigma_{e_i} = \frac{\bar{\sigma}_{v_2}}{\sqrt{2}}. \tag{21}$$

## 3 Dataset and analysis

The following two tests are carried out to assess the accuracy and reliability of the proposed method. For simplicity this new method is called AMRA-e. Specifically, test one comprises the zero and short baseline data, afterwards data of a standalone receiver is processed in test two.

### 3.1 Dataset 1—zero baseline/short baseline data

In this investigation, the performances of the zero baseline, short baseline and ARMA-e methods are analyzed and compared, especially for the new method. Data of 5 groups of dual-frequency GPS receivers are analyzed with a sampling interval of 1 s, of which group A, B and E are zero baselines and the others are short baselines. Two receivers of the same type are used in each baseline. Because the baseline lengths vary from 0 to 20 m and the time spans last from 45 to 180 min, they are sufficient to perform our analysis. Table 1 gives the details of the dataset.

In the zero and short baseline methods, the double differenced ambiguities need to be fixed firstly. In this study, the LAMBDA method is applied (Teunissen 1995; Verhagen and Li 2012), and then the single differenced residuals between receivers of each satellite are calculated by LS adjustment. The STDs of the single differenced residuals for all satellites are used as the precision estimates and are sorted in ascending order of elevations. After that, the mean precision for each elevation interval of 0.3° from 0° to 90° are computed, and the signal noise for one receiver can be estimated by dividing by $\sqrt{2}$ according to the error propagation law. Figures 1 and 2 show the relation between the signal precision and their elevation from group A to D. Precisely, Fig. 1 shows the group A and B, and Fig. 2 shows the group C and D. It can be seen that the precision of GPS signals is elevation-dependent. At the beginning, the signal precision improves with the rise of elevations. Specifically, in zero baselines, the phase precision improves from more than 1 mm to about 0.2 mm and the code precision improves from about 1 to 0.1 m. In short baselines, the precision of phase and code measurements improves from about 3 to 0.5 mm and 3 to 0.4 m, respectively. However, the precision keeps steady and even can be considered constant when the elevations are higher than 35°, as shown by the red dotted lines. The results agree with the analyses of Euler and Goad (1991) and Bona (2000). The reason is that most elevation dependent effects are eliminated above 35° elevation. In conclusion, it is possible that the majority of external effects can be eliminated in the analysis of signal precision when the satellite elevations are higher than 35°. Later discussions are based on this conclusion.

Concerning the ARMA-e method, the data of group E is illustrated firstly. For simplicity, we take the GF1 model for satellite G15 of station 1 as an example. In order to retrieve the pure random noise of the ΔGF time series, we should preprocess the ΔGF time series firstly. The GF observations and their time differenced series are shown in Figs. 3 and 4, respectively. It can be seen from Fig. 3 that the GF observations change slowly approximately from about 3.0 to 3.8 m during 45 min, since they contain the ambiguities

**Table 1** Description of the dataset

| Group name | Length (m) | Epoch numbers | Receiver type | Antenna type | Observation types |
|---|---|---|---|---|---|
| A | 0 | 10800 | JAVAD TRE_G3TH | ASH701945G_M | L1/L2/P1/P2 |
| B | 0 | 7200 | ASHTECH UZ-12 | ASH701945G_M | L1/L2/P1/P2 |
| C | 1.60 | 6300 | TRIMBLE NETR9 | LEIAR25 | L1/L2/P1/P2 |
| D | 20.04 | 7200 | LEICA GRX1200 | LEIAR25 | L1/L2/P1/P2 |
| E | 0 | 2700 | SOUTH S86 | AOAD/M_T | L1/L2/P1/P2 |

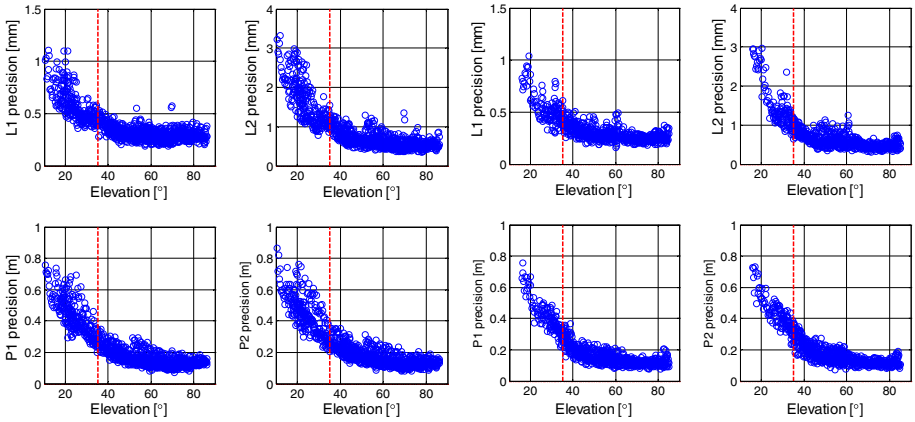


**Fig. 1** The relation between the signal precision and elevation on zero baselines of group A (*left*) and B (*right*). The *red dotted lines* denote 35° elevation. (Color figure online)

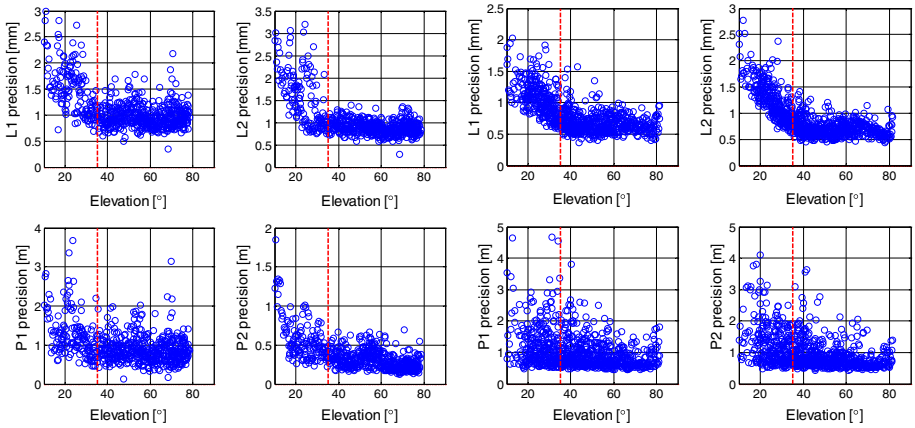


**Fig. 2** The relation between the signal precision and elevation on short baselines of group C (*left*) and D (*right*). The *red dotted lines* denote 35° elevation. (Color figure online)

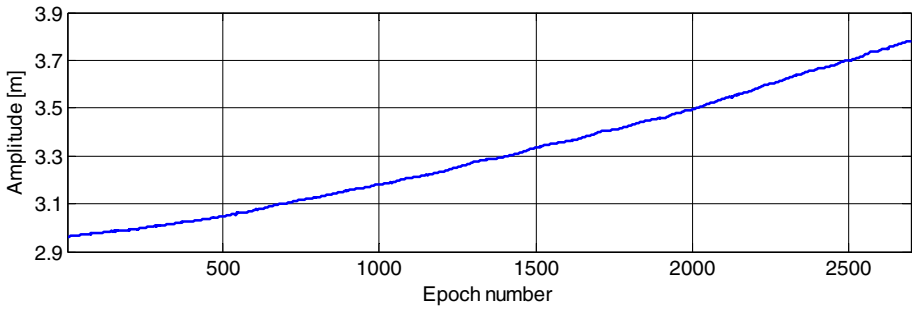


**Fig. 3** The GF observations for satellite G15 of station 1

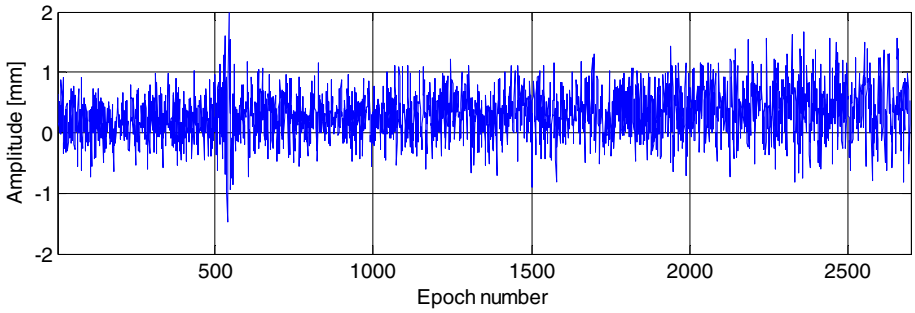


**Fig. 4** The ΔGF observations for satellite G15 of station 1

on two frequencies, ionospheric delay, multipath and hardware delays. Figure 4 shows that the ΔGF observations fluctuate between −1 and 1 mm with a slight trend. The integer ambiguities and hardware delays are removed and the ionospheric delay as well as multipath are reduced compared with the GF observations. Then the second-order polynomial fitting method and ARMA model are applied to process the time series. After that, the random noise of ΔGF is calculated which is shown in Fig. 5. It can be seen that the random noise of ΔGF is steady between −1 and 1 mm with 0 mm as the center. A closer look at Fig. 5 confirms that noise series has smaller amplitudes and are more steady than the ΔGF observations. To investigate whether the ΔGF and its noise are random, the sample autocorrelation functions are computed as shown in Fig. 6. For more details on calculating the sample autocorrelation function, see Chatfield (1984), Box et al. (1994) and Hamilton (1994). By computing a set of autocorrelation coefficients, a graph called correlogram is obtained to plot the sample autocorrelation coefficients against the lag $k$ for $k = 0,1,\ldots, m$, where $m$ is usually no more than 20. The area between the two dotted lines is the 95% confidence bounds. See the right panel of Fig. 6, 19 out of 20 of the values of autocorrelation coefficients lie between $\pm$ 0.038 (i.e.,$\pm 2/\sqrt{2700}$), therefore the ΔGF noise can be regarded random. In summary, we can draw the conclusion that the method of ARMA-e is able to effectively capture the pure random noise of ΔGF.

Similarly, the results for other satellites with elevations above 35° are also calculated. The ΔGF trends and noise are shown in Figs. 7 and 8, respectively. It can be clearly seen from Fig. 7 that the trend exhibits in ΔGF observations, of which the biggest changes in the magnitude are up to about 0.2 mm. Since the order of magnitude is equal to the phase

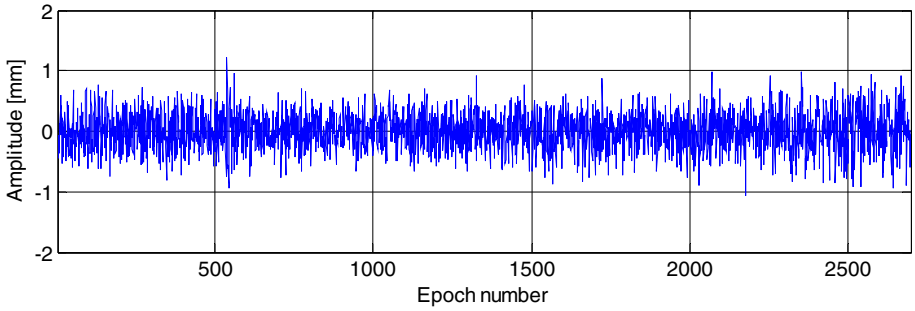


**Fig. 5** The noise of ΔGF observations for satellite G15 of station 1

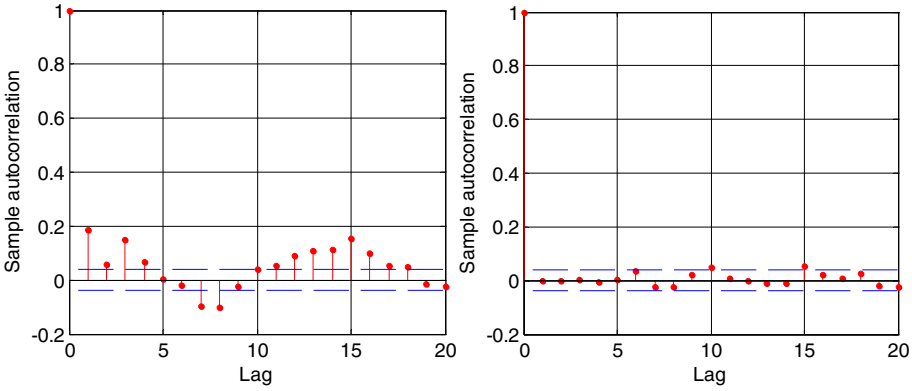


**Fig. 6** The sample autocorrelation functions of ΔGF (*left*) and its noise (*right*) for satellite G15 of station 1

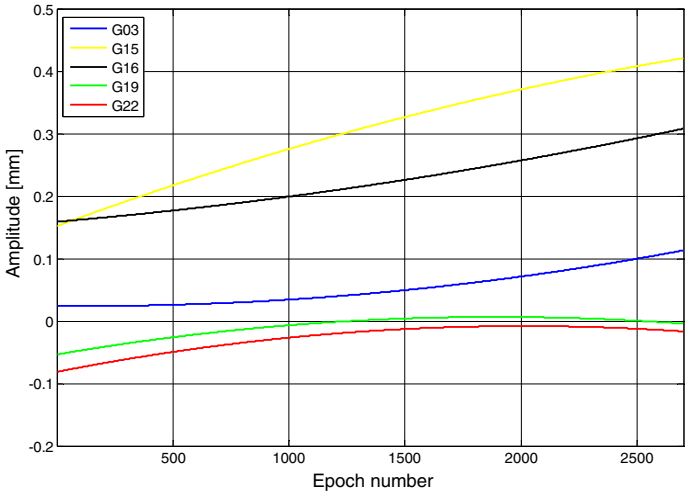


**Fig. 7** The trends of ΔGF for all satellites of station 1

noise, the detrending is required. Figure 8 shows these noise magnitudes are all vary from about −1 to 1 mm. They are similar from each other, thus indicating the reliability of the ARMA-e method. Tables 2 and 3 give the detailed results for every satellite of the two stations in group E. Judging from the parameters $p$ and $q$ of ARMA models, the mathematical model of the preprocessed ΔGF are slight different from each other. Meanwhile, it can also be found that both a mathematical correlation and a physical correlation exist in the preprocessed ΔGF model because the $p$ and $q$ are greater than 1 except for satellite G15 and G19 of station 2 in the GF2 model, which supports the findings of El-Rabbany (1994) and Howind et al. (1999) discussed before. As a result, the time correlation should be taken into account when analyzing the signal noise. At last, the measurement precision is assessed for these two receiver systems, which are given in Table 4. Compared with the results of the two stations, it can be concluded that the performance of these two receivers is almost the same.

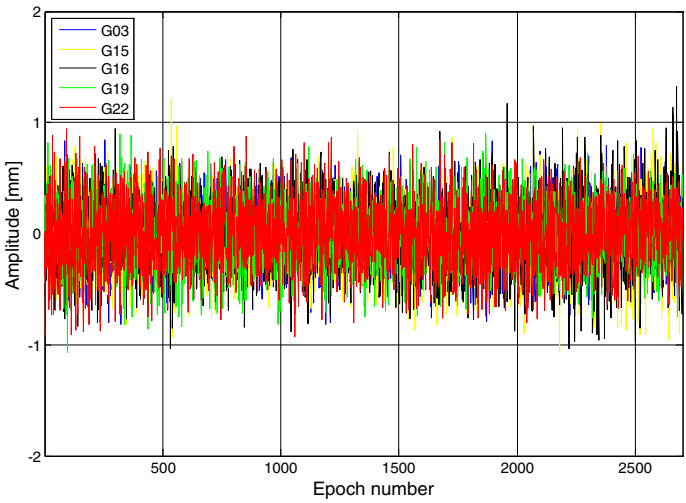


**Fig. 8** The noise of ΔGF for all satellites of station 1

**Table 2** Calculated results of station 1 with ARMA-e

| | G03 | G15 | G16 | G19 | G22 |
|---|---|---|---|---|---|
| $(p, q)$ of GF1 | (4,5) | (2,4) | (4,3) | (2,5) | (3,4) |
| $\sigma_{v_1}$(mm) | 0.263 | 0.374 | 0.319 | 0.281 | 0.295 |
| $(p, q)$ of P1 GF2 | (3,3) | (3,3) | (2,5) | (5,4) | (5,3) |
| $\sigma_{v_2}$ of P1(m) | 0.076 | 0.193 | 0.153 | 0.111 | 0.113 |
| $(p, q)$ of P2 GF2 | (1,3) | (1,3) | (4,4) | (4,5) | (5,5) |
| $\sigma_{v_2}$ of P2(m) | 0.065 | 0.195 | 0.154 | 0.102 | 0.104 |

**Table 3** Calculated results of station 2 with ARMA-e

| | G03 | G15 | G16 | G19 | G22 |
|---|---|---|---|---|---|
| $(p, q)$ of GF1 | (5,1) | (5,4) | (2,4) | (4,5) | (4,5) |
| $\sigma_{v_1}$(mm) | 0.243 | 0.372 | 0.311 | 0.269 | 0.276 |
| $(p, q)$ of P1 GF2 | (1,3) | (1,1) | (3,3) | (5,4) | (2,5) |
| $\sigma_{v_2}$ of P1(m) | 0.079 | 0.205 | 0.159 | 0.112 | 0.122 |
| $(p, q)$ of P2 GF2 | (2,2) | (4,3) | (3,3) | (1,1) | (2,4) |
| $\sigma_{v_2}$ of P2(m) | 0.067 | 0.206 | 0.157 | 0.104 | 0.114 |

**Table 4** Related results of the two receiver systems with ARMA-e

| Station | $\overline{\sigma}_{v_1}$(mm) | $\overline{\sigma}_{v_2}$ of P1(m) | $\overline{\sigma}_{v_2}$ of P2(m) | $\sigma_{\varepsilon_1}$(mm) | $\sigma_{\varepsilon_2}$(mm) | $\sigma_{e_1}$(m) | $\sigma_{e_2}$(m) |
|---|---|---|---|---|---|---|---|
| 1 | 0.306 | 0.129 | 0.124 | 0.13 | 0.17 | 0.11 | 0.10 |
| 2 | 0.294 | 0.135 | 0.130 | 0.13 | 0.16 | 0.11 | 0.11 |

In the end, we compute the GPS signal precision of each receiver for all groups using ARMA-e, zero baseline and short baseline methods. Table 5 shows the calculated results of these three methods. Firstly, the precision varies from 0.13 to 0.98 mm for phase and 0.07–0.93 m for code among these three methods. It indicates that the empirical precision of phase and code (2 mm and 0.2 m, respectively) is not realistic especially for the high-end receivers, which agrees with the conclusions of Li (2016). Secondly, in ARMA-e method, the signal precision of the two receiver systems is different from each other in group A, B, C and D, whereas only group E is not. It tells us that although two receivers share the same type, we cannot ensure the two receivers have the equal performance in real applications. Thirdly, in zero baseline method, $\sigma_{\varepsilon_1}$, $\sigma_{\varepsilon_2}$, $\sigma_{e_1}$ and $\sigma_{e_2}$ are much smaller than those in short baseline method. It indicates that the signal precision calculated for short baselines contains the unmodeled errors such as residual ionospheric biases and multipath effects.

### 3.2 Dataset 2—standalone receiver data

To analyze the stability of the ARMA-e method, the other test is carried out with data from a standalone receiver. This receiver system mainly contains two parts: the HITARGET V60 receiver and its antenna, with sampling interval of 1 s. This receiver is positioned on the rooftop or field at different times during successive 3 days. We collect the dataset during five different periods, of which the time span varies from 15 to 60 min. More details are shown in Table 6. It can be seen that the dataset has good representations and diversities. Firstly, the data are collected at different time and different locations, thus indicating a good temporal and spatial representation, respectively. Secondly, the length of observation time differs to demonstrate the applicability of the proposed method.

Figures 9 and 10 give two types of GF, ΔGF, ΔGF noise time series. As Fig. 9 shows, the GF1 observations changes slowly approximately from about −45.5 to −46.9 m mainly because of the system influences such as ambiguities on two frequencies, ionospheric delay, multipath and hardware delays. The amplitudes of the ΔGF phase observations

**Table 5** Related results of these five groups with ARMA-e, zero baseline and short baselinemethods

| Group name | Receiver system | Zero baseline/Short baseline | | | | Receiver system | ARMA-e | | | |
|---|---|---|---|---|---|---|---|---|---|---|
| | | L1 | L2 | P1 | P2 | | L1 | L2 | P1 | P2 |
| A | Rec.1 | 0.19 | 0.35 | 0.12 | 0.12 | Rec.1+Ant.1 | 0.16 | 0.21 | 0.15 | 0.15 |
| | Rec.2 | | | | | Rec.2+Ant.1 | 0.26 | 0.34 | 0.10 | 0.10 |
| B | Rec.1 | 0.21 | 0.30 | 0.11 | 0.11 | Rec.1+Ant.1 | 0.25 | 0.32 | 0.07 | 0.07 |
| | Rec.2 | | | | | Rec.2+Ant.1 | 0.15 | 0.19 | 0.12 | 0.11 |
| C | Rec.1+Ant.1 | 0.98 | 0.89 | 0.87 | 0.30 | Rec.1+Ant.1 | 0.20 | 0.25 | 0.11 | 0.11 |
| | Rec.2+Ant.2 | | | | | Rec.2+Ant.2 | 0.18 | 0.23 | 0.12 | 0.10 |
| D | Rec.1+Ant.1 | 0.67 | 0.71 | 0.93 | 0.87 | Rec.1+Ant.1 | 0.17 | 0.21 | 0.10 | 0.11 |
| | Rec.2+Ant.2 | | | | | Rec.2+Ant.2 | 0.18 | 0.23 | 0.11 | 0.11 |
| E | Rec.1 | 0.13 | 0.18 | 0.10 | 0.10 | Rec.1+Ant.1 | 0.13 | 0.17 | 0.11 | 0.10 |
| | Rec.2 | | | | | Rec.2+Ant.1 | 0.13 | 0.16 | 0.11 | 0.11 |

'Rec.' and 'Ant.' stand for the receiver and antenna respectively. *L1* and *L2* are corresponding phase precision in unit of mm. *P1* and *P2* are corresponding code precision in unit of m

**Table 6** Description of the dataset

| Number | Location | Observation time (GPS time) | Satellites to be used |
|---|---|---|---|
| No.1 | Roof | 2015/4/12 11:00:00-11:59:59 | G03 G16 G19 G23 G27 |
| No.2 | Field | 2015/4/13 04:00:00-04:59:59 | G12 G14 G18 G22 G25 |
| No.3 | Roof | 2015/4/13 11:00:00-11:29:59 | G03 G16 G19 G23 G27 |
| No.4 | Field | 2015/4/13 15:00:00-15:29:59 | G01 G07 G08 G09 G28 |
| No.5 | Roof | 2015/4/14 01:00:00-01:14:59 | G02 G05 G15 G26 G29 |

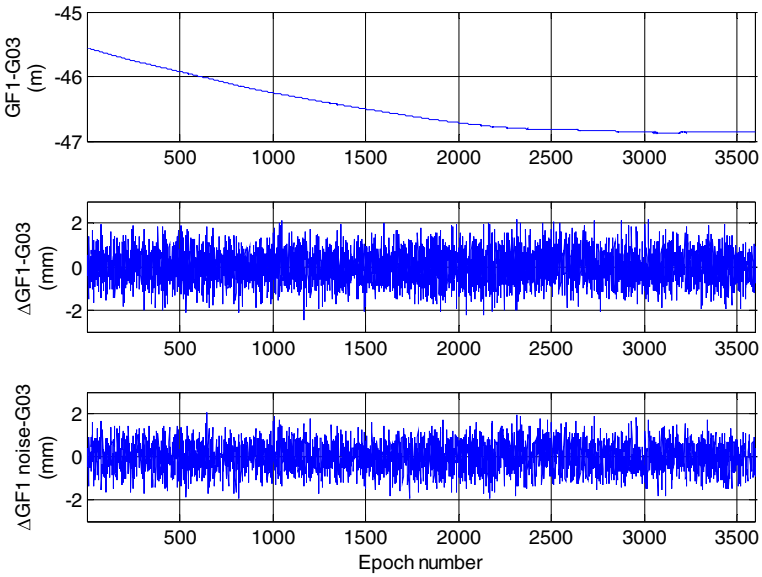


**Fig. 9** The related GF1 observations for satellite G03 of No. 1 (top the GF1 time series; middle the ΔGF1 time series; bottom the noise of ΔGF1 time series)

fluctuate between −2 and 2 mm with 0 mm as the center, which is more stable than the GF observations because there are only residual ionospheric delay and multipath left. The STD of ΔGF phase noise is 0.67 mm, but the STD of ΔGF phase observations are 0.83 mm. The reason is that the ΔGF observations have been modeled by ARMA-e method. Similar findings are valid for GF2 P1 observations as shown in Fig. 10. Table 7 shows the detailed results for the ARMA-e method of each group. It can be seen that the results are relatively consistent with each group. More specifically, the precision differences of L1, L2, P1 and P2 between the maximum and minimum among these five groups are 0.03, 0.03 mm, 0.02 and 0.01 m, respectively. Therefore, the results of different groups can be treated equal. Accordingly, the noise of this receiver system can be computed, where the precision of L1, L2, P1 and P2 are 0.33, 0.43 mm, 0.22 and 0.17 m respectively. In summary, we can see that the precision of phase and code noise is almost the same even for different observation times and locations. This indicates that our method is robust since it is independent of the external environment.

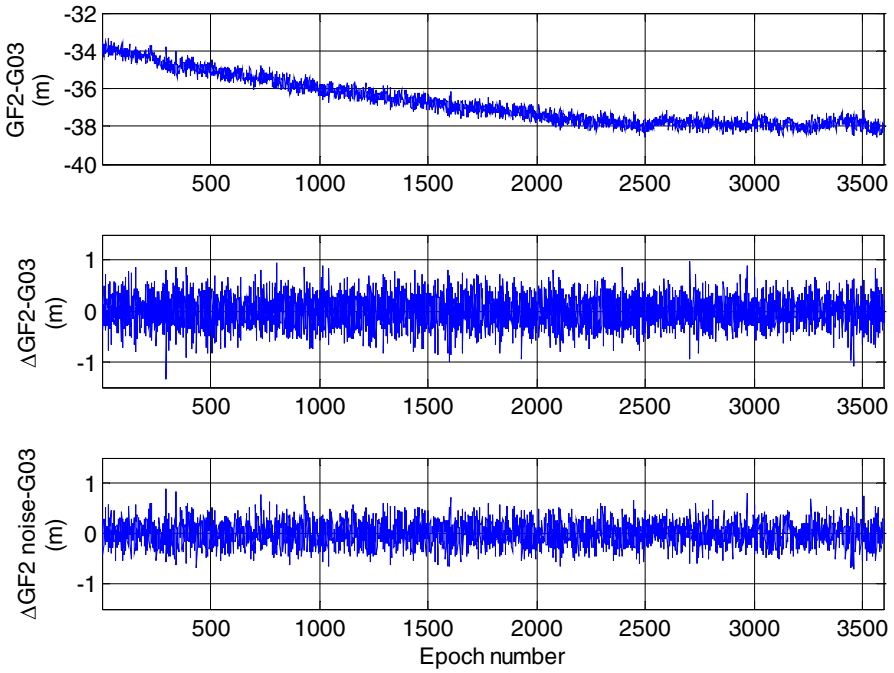


**Fig. 10** The related GF2 P1 observations for satellite G03 of No. 1 (top the GF2 time series; middle the ΔGF2 time series; bottom the noise of ΔGF2 time series)

**Table 7** Phase and code precision of the HITARGET V60 receiver system

| Group | L1(mm) | L2(mm) | P1(m) | P2(m) |
|---|---|---|---|---|
| No.1 | 0.33 | 0.42 | 0.21 | 0.17 |
| No.2 | 0.35 | 0.45 | 0.23 | 0.18 |
| No.3 | 0.32 | 0.42 | 0.21 | 0.17 |
| No.4 | 0.35 | 0.45 | 0.23 | 0.17 |
| No.5 | 0.32 | 0.42 | 0.23 | 0.17 |

## 4 Concluding remarks

This paper develops an alternative noise assessment method useful for standalone GPS receiver system. To obtain the receiver signal precision, the ARMA model is applied to get rid of mathematical and physical correlations in detrended ΔGF time series.

Since the new method focuses on single receiver system (i.e., one receiver and one antenna) without external impacts, it is especially suitable to be applied for PPP receivers. However, this method requires dual frequency or triple frequency measurements, limiting its practical applications to some extent. In essential, this method can be transformed easily to process other types of data, such as GLONASS, Galileo and BeiDou signals, which is useful in multi-constellation PPP when setting up the stochastic model.

**Acknowledgements** This study is sponsored by The National Key Research and Development Program of China (2016YFB0501802), The National Natural Science Funds of China (41574023, 41374031) and The National Natural Science Foundation of China (41622401). The second author is also supported by the Fund

of Youth 1000-Plan Talent Program of China. The reviewers and editors are acknowledged for their constructive comments.

## References

Afifi A, El-Rabbany A (2013) Stochastic modeling of Galileo E1 and E5a signals. Int J Eng Innov Technol IJEIT 3:188–192

Amiri-Simkooei A, Tiberius C (2007) Assessing receiver noise using GPS short baseline time series. GPS Solut 11:21–35

Bona P (2000) Precision, cross correlation, and time correlation of GPS phase and code observations. GPS Solut 4:3–13

Bona P, Tiberius C (2000) An experimental comparison of noise characteristics of seven high-end dual frequency GPS receiver-sets. In: Position location and navigation symposium, IEEE 2000, IEEE, pp 237–244

Box GE, Jenkins GM, Reinsel GC, Ljung GM (1994) Time series analysis: forecasting and control. Wiley, Hoboken

Chatfield C (1984) The analysis of time series: an introduction. CRC Press, Boca Raton

de Bakker PF, van der Marel H, Tiberius CC (2009) Geometry-free undifferenced, single and double differenced analysis of single frequency GPS, EGNOS and GIOVE-A/B measurements. GPS Solut 13:305–314

de Bakker PF, Tiberius CC, van der Marel H, van Bree RJ (2012) Short and zero baseline analysis of GPS L1 C/A, L5Q, GIOVE E1B, and E5aQ signals. GPS Solut 16:53–64

El-Rabbany A (1994) The effect of physical correlations on the ambiguity resolution and accuracy estimation in GPS differential positioning. Department of Geodesy and Geomatics Engineering, University of New Brunswick, Fredericton

Euler H, Goad C (1991) On optimal filtering of GPS dual frequency observations without using orbit information. Bull Geod 65:130–143

Ge M, Gendt G, Rothacher M, Shi C, Liu J (2008) Resolution of GPS carrier-phase ambiguities in precise point positioning (PPP) with daily observations. J Geod 82:389–399

Hamilton J (1994) Time series analysis. Princeton University Press Princeton, Princeton

Han S (1997) Quality-control issues relating to instantaneous ambiguity resolution for real-time GPS kinematic positioning. J Geod 71:351–361

Hofmann-Wellenhof B, Lichtenegger H, Wasle E (2007) GNSS–global navigation satellite systems: GPS, GLONASS, Galileo, and more. Springer Science & Business Media

Howind J, Kutterer H, Heck B (1999) Impact of temporal correlations on GPS-derived relative point positions. J Geod 73:246–258

Langley RB (1997) GPS receiver system noise. GPS World 8:40–45

Leick A, Rapoport L, Tatarnikov D (2015) GPS satellite surveying. Wiley, Hoboken

Li B (2016) Stochastic modeling of triple-frequency BeiDou signals: estimation, assessment and impact analysis. J Geod 90:1–18

Nolan J, Gourevitch S, Ladd J (1992) Geodetic processing using full dual band observables. Proc IONGPS 92:1033–1041

Rodríguezpérez JR, Álvarez MF, Sanzablanedo E (2007) Assessment of low-cost GPS receiver accuracy and precision in forest environments. J Surv Eng 133:159–167

Schwarz G (1978) Estimating the dimension of a model. Ann Stat 6:461–464

Teunissen P (1995) The least-squares ambiguity decorrelation adjustment: a method for fast GPS integer ambiguity estimation. J Geod 70:65–82

Tiberius C, De Bakker P, Marel H, van Bree R (2001) Geometry-free analysis of GIOVE-A/B E1-E5a, and GPS L1-L5 measurements. In: Proceedings of the 22nd international technical meeting of the satellite division of the institute of navigation (ION GNSS 2009), pp 2911–2925

Van der Marel H, de Bakker P, Tiberius C (2009) Zero, single and double difference analysis of GPS, EGNOS and GIOVE-A/B pseudorange and carrier phase measurements. In: Proceedings of ENC GNSS

Verhagen S, Li B (2012) LAMBDA software package: Matlab implementation, version 3.0. Delft University of Technology and Curtin University, Perth, Australia

Wang J, Satirapod C, Rizos C (2002) Stochastic assessment of GPS carrier phase measurements for precise static relative positioning. J Geod 76:95–104

Welford B (1962) Note on a method for calculating corrected sums of squares and products. Technometrics 4:419–420
Zumberge J, Heflin M, Jefferson D et al (1997) Precise point positioning for the efficient and robust analysis of GPS data from large networks. J Geophys Res Solid Earth 1978–2012(102):5005–5017